




Lanczos-Pascal approach to correlation functions in chaotic quantum systems

Merlin Füllgraf ^{1,*}, Jiaozi Wang ¹ and Jochen Gemmer ^{1,†}

¹*University of Osnabrück, Department of Mathematics/Computer Science/Physics, D-49076 Osnabrück, Germany*
(Dated: March 25, 2025)

Equilibration is a ubiquitous phenomenon in chaotic quantum systems. Given the variety and multitude of condensed matter-type chaotic quantum systems, it may be considered as surprising how simple dynamics often are on the level of few body observables. In the context of this paper *simple* implies "in good agreement with a superposition of only a few exponentially damped oscillations". We follow the (possibly somewhat odd) idea that it may be precisely the complexity of chaotic systems that entails the simpleness of their dynamics. We do so employing the framework of the recently resurged recursion method comprising Lanczos coefficients to generate the dynamics. We find that the structure of the Lanczos coefficients that enables simpleness is in accord with the *operator growth hypothesis*. We present a method to explicitly construct approximations to the dynamics from the Lanczos coefficients. These approximations result as *simple* for various chaotic spin systems. While the consideration applies to systems in the thermodynamic limit, we compare our approximations to state-of-the-art numerics for large but finite quantum systems and obtain good agreement.

I. INTRODUCTION

The emergence of thermodynamical behavior and irreversibility in quantum systems from microscopically time-symmetric equations of motion remains a lively investigated line of research to this day. In closed quantum systems, concepts like the eigenstate thermalization hypothesis (ETH) and quantum typicality are cornerstones for the theory of thermalization of observables [1–3]. For the actual dynamical properties in the equilibration of the observables, e.g. captured by (auto)correlation functions, no such concepts exist in such generality. Still, oftentimes nature appears to favor certain classes of dynamics over others, resulting in a magnitude of examples, e.g. featuring exponential relaxation or damped oscillations [4, 5].

It has been pointed out in the literature that exponentials (with possibly complex exponents) play an important role in the relaxation dynamics of chaotic systems, especially in the long time limit. This is known under the name of Ruelle-Pollicot resonances or pseudomode expansion or (approximate) dynamical symmetries [6–9]. The present paper is in line with these concepts but goes substantially further beyond with respect to the above simpleness of the dynamics. It may also be worth pointing out that our approach does not rely on any weak coupling or timescale separation argument.

In principle, for functions with an existing Laplace transform, the existence of a representation in terms of arbitrarily many exponentials is ensured. Yet, from a conceptual point of view, in order to investigate natures apparent soft spot for simple dynamics, it is desirable to investigate the possibility to decompose the dynamics into few simple constituents. Concretely, we focus

on the question whether for pertinent chaotic quantum systems, the equilibration dynamics of few-body observables can be expected to be *simple*, in the above sense. To this end, we investigate the dynamics of an observable in operator space with the framework of the so-called recursion method. In operator space, the dynamics are imposed by the Liouvillian superoperator, defined by the Hamiltonian \mathcal{H} as $\mathcal{L} = [\mathcal{H}, -]$.

Our approach comprises a method to truncate the Liouvillian in order to add "dissipation" to the otherwise unitary dynamics. This truncation is moderated by a so-called *truncation vector* \vec{s} . We motivate our truncation vector \vec{s} as a discrete differential operator on a sequence calculated from the Lanczos coefficients. The principle ansatz to truncate the Liouvillian by means of a truncation vector has been mentioned in Ref. [10] and recently appeared as a central concept in Ref. [9]. However, whereas already in Ref. [10], the necessity of smoothness in the associated tight-binding model was assumed, so far no encompassing theory, explaining the expected applicability of such a scheme has been developed (to our knowledge).

We compute an approximation to the actual correlation function in terms of a fixed (small) number of damped oscillations for some examples. We then compare the curves, and by that the accuracy of our method, to results from state-of-the-art numerics.

Furthermore, we construct a necessary *a priori*-criterion for the convergence of our scheme on the basis of the Lanczos coefficients.

II. SETTING

There are several equivalent ways to describe the dynamics in closed systems; each with distinct advantages and limitations. In this work we focus on the dynamics being defined by the so-called Lanczos coefficients b_n ; a set of real positive number uniquely defining the auto-

* merlin.fuellgraf@uos.de

† jgemmer@uos.de

correlation function $C(t)$ of a given observable and vice versa. Therefore we briefly revisit this setting.

Given a Hamiltonian \mathcal{H} and an observable \mathcal{O} , we consider the autocorrelation function at infinite temperature defined by

$$C(t) = \text{tr}\{e^{i\mathcal{H}t}\mathcal{O}e^{-i\mathcal{H}t}\mathcal{O}\}/d, \quad (1)$$

with d the Hilbert space dimension. Denoting the elements of the operator space by $|\mathcal{O}\rangle$, the Hilbert-Schmidt scalar product reads $(\mathcal{A}|\mathcal{B}) := \text{tr}\{\mathcal{A}^\dagger\mathcal{B}\}/d$. The Liouvillian $\mathcal{L}(-) := [\mathcal{H}, -]$ generates the time-evolution via $|\mathcal{O}(t)\rangle = \exp(i\mathcal{L}t)|\mathcal{O}\rangle$ such that the autocorrelation functions takes the form $C(t) = (\mathcal{O}|\exp(i\mathcal{L}t)|\mathcal{O})$. The Lanczos algorithm then starts from a normalized vector $|\mathcal{O}_0\rangle =: |\mathcal{O}\rangle$ and produces Lanczos coefficients b_n and Krylov vectors $|\mathcal{O}_n\rangle$ as

$$\begin{aligned} |\tilde{\mathcal{O}}_n\rangle &= \mathcal{L}|\mathcal{O}_{n-1}\rangle - b_{n-1}|\mathcal{O}_{n-2}\rangle \\ b_n &= (\tilde{\mathcal{O}}_n|\tilde{\mathcal{O}}_n)^{1/2} \\ |\mathcal{O}_n\rangle &= b_n^{-1}|\tilde{\mathcal{O}}_n\rangle, \end{aligned} \quad (2)$$

with b_0 . Further, we define the real functions

$$\varphi_n(t) := i^{-n}(\mathcal{O}_n|\mathcal{O}(t)) \quad (3)$$

that inherit the Schrödinger equation from (2) as

$$\partial_t \varphi_n(t) = b_n \varphi_{n-1}(t) - b_{n+1} \varphi_{n+1}(t) \quad \text{for } n \geq 0, \quad (4)$$

with initial condition $\varphi_n(0) = \delta_{n,0}$. This equation may equivalently be written as a matrix equation

$$\dot{\vec{\varphi}} = \mathbf{L} \cdot \vec{\varphi}, \quad (5)$$

where the matrix \mathbf{L} is given by

$$\mathbf{L} = \begin{pmatrix} 0 & -b_1 & 0 & 0 & \dots \\ b_1 & 0 & -b_2 & 0 & \dots \\ 0 & b_2 & 0 & -b_3 & \dots \\ 0 & 0 & b_3 & 0 & \dots \\ \vdots & \vdots & \vdots & \vdots & \ddots \end{pmatrix}, \quad (6)$$

and where $(\vec{\varphi})_n = \varphi_n$. With the Schrödinger equation in line (4) the Lanczos coefficients may be seen as hopping amplitudes of a particle on a semi-infinite lead, the Mori chain. Therefore we refer to $\vec{\varphi}(t)$ as wave function or wave vector while its entries $\varphi_n(t)$ may be interpreted as amplitudes of the particle being located at site n with probability $\varphi_n^2(t)$.

Given an infinite number of Lanczos coefficients, the autocorrelation function can be obtained as the solution of the matrix equation (5). In practice, however, only a finite number (mostly in the lower two-digit regime) of Lanczos coefficients is numerically feasible. Subsequent b_n are typically extrapolated by means of the universal operator growth hypothesis (OGH) [11]. The latter states that in infinite non-integrable many-body systems the Lanczos coefficients of a local observable asymptotically exhibit linear growth (with logarithmic corrections in one dimension). Oftentimes already the first several numerically obtained Lanczos coefficients exhibit a

linear behavior. Whether this precise trend (as manifested in slope and offset) persists for later n is a priori not certain. For instance the OGH also allows for the asymptotic trend to appear well beyond the numerical scope. For pertinent physical properties these subtle questions are typically of subordinate importance and a linear continuation on the basis of the accessible Lanczos coefficients is a well-accepted way approximate the dynamics of $C(t)$. Turning back to the matrix equation (5), any finite-dimensional $d \times d$ matrix \mathbf{L} will yield $d/2$ complex-conjugate pairs of eigenvalues (if d is odd, there are $\frac{d-1}{2}$ pairs and one vanishing eigenvalue) by the skew-hermiticity of \mathbf{L} . Consequently, the solution for $C(t)$ will be a superposition of oscillating terms and therefore inevitably exhibit *echoes*.

III. LANCZOS-PASCAL APPROACH

In this work we aim to present a cheap yet remarkably/notably accurate scheme to approximate autocorrelation functions by means of only the numerically accessible Lanczos coefficients under rather mild conditions on the inaccessible ones. Let \mathbf{L} to this end be again the infinite-dimensional matrix defined in (5) with the solution $\vec{\varphi}(t)$. Further we denote by \mathbf{P}_R the projector onto the first R components of $\vec{\varphi}(t)$. Let \mathbf{L}_R denote an $R \times R$ matrix which satisfies

$$\mathbf{P}_R \dot{\vec{\varphi}}(t) = \mathbf{L}_R \vec{\varphi}(t) = \mathbf{P}_R \mathbf{L} \mathbf{P}_R \vec{\varphi}(t). \quad (7)$$

If such a matrix exists then it generates the first R components of $\vec{\varphi}(t)$ correctly. In order to determine \mathbf{L}_R we may write

$$\mathbf{L}_R \vec{\varphi} = \mathbf{P}_R \dot{\vec{\varphi}} = \mathbf{P}_R \mathbf{L} \vec{\varphi} \quad (8)$$

$$\Rightarrow (\mathbf{L}_R - \mathbf{P}_R \mathbf{L}) \vec{\varphi} = 0. \quad (9)$$

For the sake of explicitness we consider the case of $R = 3$ in detail. Our ansatz is to choose \mathbf{L}_R as

$$\mathbf{L}_R = \begin{pmatrix} 0 & -b_1 & 0 \\ b_1 & 0 & -b_2 \\ b_3 k_0 & b_2 + b_3 k_1 & b_3 k_2 \end{pmatrix}, \quad (10)$$

with real constants k_0, k_1, k_2 . Turning back to Eq. (9) we have

$$\mathbf{L}_R - \mathbf{P}_R \mathbf{L} = \begin{pmatrix} 0 & 0 & 0 & 0 \\ 0 & 0 & 0 & 0 \\ b_3 k_0 & b_3 k_1 & b_3 k_2 & b_3 \end{pmatrix} \quad (11)$$

such that with Eq. (9) we arrive at

$$b_3 (k_0 x_0 + k_1 x_1 + k_2 x_2 + 1 \cdot x_3) = 0. \quad (12)$$

Hence the search of an appropriate \mathbf{L}_R is equivalent to that of a vector $\vec{s} = (k_0, k_1, k_2, k_3 = 1)^T$ perpendicular to $\vec{\varphi}$, i.e.

$$\vec{s} \cdot \vec{\varphi} = 0. \quad (13)$$

By allowing for different dimensions R , our approach yields an approximation to the actual autocorrelation function that by construction consists of $R/2$ damped oscillations. Therefore it is reasonable to expect that in principle, the agreement becomes better as more Lanczos coefficients are taken into account and the approximation consists of oscillations. However, again our aim is to suitably describe the dynamics by as few constituents possible, addressing the observation that generally, for complex chaotic systems, the dynamics are typically simple.

Clearly, the details of the approximation are captured in the structure of the truncation vector \vec{s} . We construct our truncation vector as

$$s_{m+j} = (-1)^{O+j} \binom{O}{j}, \quad \text{where } 0 \leq j \leq O \quad (14)$$

and $1 \leq O \leq R - m$,

where m denotes the left edge of the truncation vector, and O an as of now free parameter. Consider a given 4×4 matrix \mathbf{L}_R ; there are 4 different possible truncation vectors

$$\vec{s} = \begin{cases} (0 & 0 & 0 & -1 & | & 1)^T \\ (0 & 0 & 1 & -2 & | & 1)^T \\ (0 & -1 & 3 & -3 & | & 1)^T \\ (1 & -4 & 6 & -4 & | & 1)^T, \end{cases} \quad (15)$$

where we indicated the components k_j from $\vec{s} = (\vec{\mathbf{k}}, 1)^T$. In what follows we shall refer to O as the order of the truncation vector, starting from one which for the case of $R = 4$ corresponds to the first line in Eq. (14). Note that the entries of Eq. (14) may be seen as rows of Pascal's triangle with alternating sign. Hence we refer to this scheme as *Lanczos-Pascal* (LP) approach.

Next, we formulate a necessary criterion for the convergence of the LP scheme. When taking subsequently more Lanczos coefficients into account (until a maximum of $M = n_{\max}$), the area under the curve of each approximation needs to converge with increasing M (strictly this approach is only well defined if the areas themselves are finite). For the sake of clarity we illustrate this argument for a fixed size $R = 4$ stressing that the line of reasoning holds true for arbitrary R . Consider

$$\dot{\vec{\varphi}} = \underbrace{\begin{pmatrix} 0 & -b_1 & 0 & 0 \\ b_1 & 0 & -b_2 & 0 \\ 0 & b_2 & 0 & -b_3 \\ b_4 k_0 & b_4 k_1 & b_3 + b_4 k_2 & b_4 k_3 \end{pmatrix}}_{\mathbf{L}_R} \cdot \vec{\varphi} \quad (16)$$

with initial condition $\vec{\varphi}(0) = (1, 0, 0, 0)^T$. Upon performing a Laplace transform we get

$$\begin{pmatrix} -1 \\ 0 \\ 0 \\ 0 \end{pmatrix} = \mathbf{L}_R \begin{pmatrix} \tilde{\varphi}_0(0) \\ \tilde{\varphi}_1(0) \\ \tilde{\varphi}_2(0) \\ \tilde{\varphi}_3(0) \end{pmatrix}, \quad (17)$$

where $\tilde{\varphi}_k(0)$, hereafter abbreviated by $\tilde{\varphi}_k$, denotes the Laplace transform of the k th entry of the wave vector $\vec{\varphi}$ at zero. Crucially, the Laplace transform of the (approximated) autocorrelation function evaluated at zero corresponds to the area \mathcal{A} under the respective curve, $\tilde{\varphi}_0 = \mathcal{A}$. Analogous to Eq. (12) and with $\tilde{\varphi}_{2n} =: v_{2n} \tilde{\varphi}_0$ we find

$$0 = k_0 v_0 \tilde{\varphi}_0 + k_1 \tilde{\varphi}_1 + \left(\frac{b_3}{b_4} + k_2 \right) v_2 \tilde{\varphi}_0 + k_3 \tilde{\varphi}_3 \quad (18)$$

$$0 = k_0 \tilde{\varphi}_0 + k_1 \tilde{\varphi}_1 + k_2 \tilde{\varphi}_2 + k_3 \tilde{\varphi}_3 + k_4 \tilde{\varphi}_4 \quad (19)$$

$$0 = \vec{\mathbf{k}}_{\text{even}} \cdot \vec{\mathbf{v}} \tilde{\varphi}_0 + \vec{\mathbf{k}}_{\text{odd}} \cdot \vec{\mathbf{u}} \quad (20)$$

$$\Leftrightarrow \tilde{\varphi}_0 = \frac{-\vec{\mathbf{k}}_{\text{odd}} \cdot \vec{\mathbf{u}}}{\vec{\mathbf{k}}_{\text{even}} \cdot \vec{\mathbf{v}}}, \quad (21)$$

with $\vec{\mathbf{k}}_{\text{even/odd}}$ containing only k_j with even/odd j and both $\vec{\mathbf{v}}, \vec{\mathbf{u}}$ as vectors with entries v_j and $u_j = \tilde{\varphi}_j$ (with j odd) respectively, and where we used that $u_4 = \frac{b_3}{b_4} u_2$ (as to be inferred from the below (22) such that with $k_{R+1=4} = 1$ (as in the definition of \vec{s} below Eq. (12)) we may condense the denominator of Eq. (21). Several remarks are in order. First, with some algebraic transformations, from Eq. (17) we may express any $\tilde{\varphi}_j$ with j odd as a product of Lanczos coefficients, e.g.

$$u_{j=1,3,5,\dots} = \frac{1}{b_1}, \frac{1}{b_1 b_3}, \frac{1}{b_1 b_3 b_5}, \dots \quad (22)$$

Secondly, for even j the coefficients u_j take a similar form

$$v_{0,2,4,\dots} = 1, \frac{b_1}{b_2}, \frac{b_1 b_3}{b_2 b_4}, \dots \quad (23)$$

Considering (19) we may infer that for our choice of \vec{s} the sequence $\tilde{\varphi}_0$ the equation will only be well fulfilled if this sequence is "smooth" in the respective regime, since the construction $\vec{s} \cdot \dots$ amounts to taking a derivative with respect to n of order O . The existence of this smoothness depends on the b_n . If it is present for $n \geq r$, (21) will hold with a fixed $\tilde{\varphi}_0$ independent of m and O for all $m \geq r$.

To rephrase, positioning the truncation vector $\vec{\mathbf{k}}$ within a region of suitably linear/smooth Lanczos coefficients we may expect the area under the respective (approximation to the) autocorrelation function to converge while taking successively more Lanczos coefficients into account. Moreover, having fixed the structure of the truncation vector \vec{s} , e.g. by fixing the order O , monitoring Eq. (21) along the number of considered Lanczos coefficients b_n , serves as an *a priori* indicator for the convergence of the LP scheme. Furthermore, let us revisit the smoothness $\tilde{\varphi}_n$ that induces the above convergence. (Note that for even n , the $\tilde{\varphi}_n$ have a "free" multiplicative parameter, $\tilde{\varphi}_0$.) In order for adjacent u_k, v_{k+1} to possibly be aligned into a smooth sequence $\tilde{\varphi}_n$, the Lanczos coefficients nec-

essarily need to fulfill

$$\frac{b_n}{b_{n+1}} \approx \frac{b_{n-1}}{b_n} \left(\approx \frac{b_{n-2}}{b_{n-1}} \right) \quad (24)$$

$$\Leftrightarrow 1 \approx \frac{b_{n-1}b_{n+1}}{b_n^2}. \quad (25)$$

Furthermore, considering

$$\frac{b_n}{b_{n+1}} \approx \frac{b_{n-2}}{b_{n-1}} \quad (26)$$

yields that consequently the sequences u_k, v_k themselves are smooth. We may also check the consistency of the smoothness argument by checking the \mathcal{A} that results from it. Smoothness requires that all adjacent $\tilde{\varphi}_n$ are very similar. For example we may require that the last odd $\tilde{\varphi}_n$ coincides with its predecessor. For the precise case formulated in Eq. (21) this amounts to

$$\tilde{\varphi}_2 \stackrel{!}{=} \tilde{\varphi}_3 \Leftrightarrow \tilde{\varphi}_0 \frac{b_1}{b_2} = \frac{b_2}{b_1 b_3} \quad (27)$$

$$\Leftrightarrow \tilde{\varphi}_0 = \frac{b_2^2}{b_1^2 b_3}. \quad (28)$$

Equation (28) itself describes an approximation to the area under the curve, cf. [12, 13]. To conclude this section we point out (and stress) that the validity of the condition (25) above some n is in line with the OGH. In Fig. 1 we exemplarily check the condition (25) and depict the sequences u_k, v_k as well as the aligned sequence for a physical model investigated in Sec. IV.

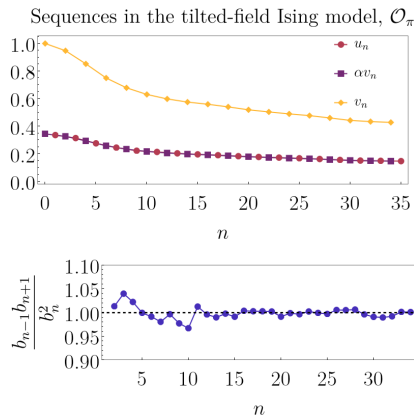


FIG. 1. **Top:** Sequences (u_n) and (v_n) for the Lanczos coefficients of the fast-mode of the energy-density wave operator (32) in the tilted-field Ising model (31). Upon multiplying by a factor α , obtained similarly to Eq. (28), we may render the sequence (φ_n) smooth. **Bottom:** Numerical check of condition (25) for the same model and observable.

IV. NUMERICS

A priori the order O of the truncation vector $\vec{\mathbf{k}}$ remains an open parameter. Typically, for physical models only a

lower two-digit number of Lanczos coefficients is numerically feasible. Upon unsystematic varying of the free parameter O , we suggest to fix the order of $\vec{\mathbf{k}}$ in relation to the number of considered Lanczos coefficients R as

$$O = \lfloor \frac{R}{4} \rfloor, \quad (29)$$

where by $\lfloor - \rfloor$ we denote the floor function. It is important to stress again that the scope of this paper is to present a cheap, yet reasonably accurate technique to approximate autocorrelation functions based on few Lanczos coefficients. Neither do we claim our choice to be optimal with respect to the structure of the truncation vector nor the precise order, as suggested in Eq. (29). In the following numerical section however, we aim to convey the somewhat surprising numerical accuracy of this rather cheap technique, advocating the usefulness of our construction.

Toy model. One of the few examples in which both the Lanczos coefficients as well as a closed form of the autocorrelation function are known is given by

$$b_n = n \longleftrightarrow C(t) = \operatorname{sech} t, \quad (30)$$

see e.g. [14]. The scenario of purely linear Lanczos coefficients serves as a first indicator for the quality of the truncation scheme. Similar to the general scenario, in which only a limited number of Lanczos coefficients is available, we restrict ourselves to consider only 50 Lanczos coefficients. Employing our suggestion (29) to fix the order O , we investigate the areas \mathcal{A}_R when taking an increasing number R of Lanczos coefficients into account. As a cheap indicator, hinting on a convergence with respect to R , we determine the number n after which the areas \mathcal{A}_n vary less than $1/200 \max_j \mathcal{A}_j$ from adjacent areas, see Fig. 2. For the case of linear Lanczos and the convention (29), we find this to be the case at $R = 8$. In Fig. 2 we depict the first non-trivial approximation to $C(t)$, $R = 2$, along with the first approximation that meets the above convergence criterion for \mathcal{A} , $R = 8$, as well as the actual analytical autocorrelation function $C(t) = \operatorname{sech} t$. We see that while for $R = 2$ the approximation clearly differs from the actual autocorrelation function, the LP scheme is able to construct an approximation consisting of only four damped oscillations that matches the autocorrelation remarkably well, even on the log-scale.

A. Physical models

We consider several pairs of physical models \mathcal{H} and observables \mathcal{O} numerically. For each pair we infer a maximal number of feasible n_{\max} Lanczos coefficients. This number depends on the structure of \mathcal{H} and \mathcal{O} alike. Again, we aim to approximate the dynamics of the autocorrelation function in terms of few damped oscillations on the basis of the available Lanczos coefficients and the truncation vector $\vec{\mathbf{k}}$. In order to have a meaningful notion

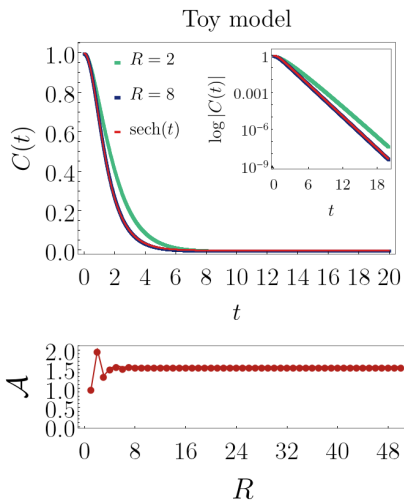


FIG. 2. **Top:** Comparison of the analytical form of $C(t)$ in the setting of linear Lanczos coefficients against the approximation from the LP scheme. **Bottom:** The areas under the curve for the curves from the LP scheme for different numbers R of considered Lanczos coefficients.

of *true* dynamics we compare the approximation with curves obtained by state-of-the-art numerical methods. For the LP scheme proceed as follows:

For every observable we track the area \mathcal{A}_R under the curve for different numbers of considered Lanczos coefficients R up to a maximum n_{\max} . We then display the first approximation that is not purely exponential by construction, $R = 2$, as well as the curve with minimal R satisfying the above introduced convergence criterion. This is the *simplest* curve we determine (in the sense of a superposition of few simple constituents) whose area has converged within our scope. Additionally we display the case with $R = n_{\max}$.

Tilted field Ising model. As a first representative of a generic quantum many-body system, we consider a tilted field Ising model, described by the Hamiltonian

$$\mathcal{H} = \sum_k \sigma_k^x \sigma_{k+1}^x + \frac{B_z}{2} (\sigma_k^z + \sigma_{k+1}^z) + \frac{B_x}{2} (\sigma_k^x + \sigma_{k+1}^x), \quad (31)$$

with $(B_x, B_z) = (1.05, 0.5)$. For this model we investigate four different observables, altogether arguing for the universality and generic nature of our findings. First, we consider the density-wave operator of the energy

$$\mathcal{O}_q \propto \sum_k \cos(qk) h_k. \quad (32)$$

Here, h_k denotes the local energy, given by the addend in the sum in Eq. (31). For this observable we focus on both a fast as well as a slow mode, represented by $q = \pi$ and $q = \pi/12$ respectively. Next, we include the two-local

observable

$$\mathcal{B} \propto \sum_k 1.05 \sigma_k^x \sigma_{k+1}^x + \sigma_k^z \quad (33)$$

into our examination. This observable is special as it is orthogonal to the Hamiltonian, $(\mathcal{B}|\mathcal{H}) = 0$. As a fourth observable, we consider the energy current

$$\mathcal{J}_E = B_x \sum_k \sigma_k^y (\sigma_{k+1}^z - \sigma_{k-1}^z). \quad (34)$$

For every observable we determine a number of n_{\max} numerically feasible Lanczos coefficients. Concretely, for the density-wave operators \mathcal{O}_q and the two-local observable \mathcal{B} we compute 40 Lanczos coefficients and for the energy current \mathcal{J}_E we infer 44. In order to benchmark, we use dynamical quantum typicality techniques [15] and study the respective finite system of size $L = 28$ with periodic boundary conditions.

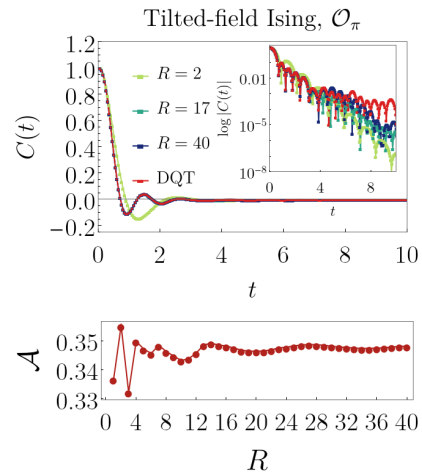


FIG. 3. **Top:** Comparison of the LP curves for the fast mode of the energy density-wave observable \mathcal{O}_π in the tilted-field Ising model against DQT data for the finite system with $L = 28$. **Bottom:** The areas under the curve of the LP approximation for different R . Here we find convergence at $R = 17$.

For any of the investigated observables we find a remarkably good agreement of the LP method with the exact curves obtained by DQT for the finite system with $L = 28$ and periodic boundary conditions. Especially for the observables \mathcal{O}_π , $\mathcal{O}_{\pi/12}$ and \mathcal{B} the accuracy is pronounced, even on the log-scale. Here, visible deviations occur only on a scale on which the DQT error becomes non-negligible. Practically, all autocorrelation functions are captured by ~ 10 damped oscillations. In the case of the energy current \mathcal{J}_E the picture is slightly different. Whereas again, to the naked eye, the agreement of the LP approach and the DQT curve is good on the short-time scale, the LP curve does not fully capture the long-time behavior of the autocorrelation function. This

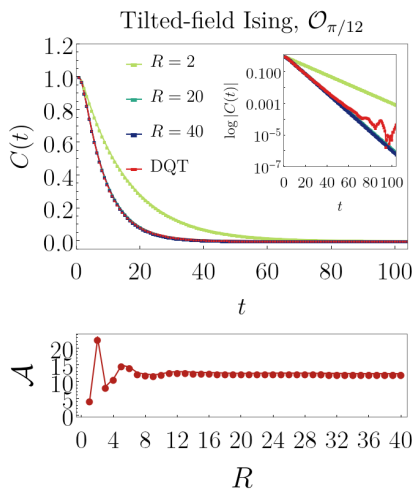


FIG. 4. **Top:** Comparison of the LP curves for the slow mode of the energy density-wave observable $\mathcal{O}_{\pi/12}$ in the tilted-field Ising model against DQT data for the finite system with $L = 28$. **Bottom:** The areas under the curve of the LP approximation for different R . Here we find convergence at $R = 20$.

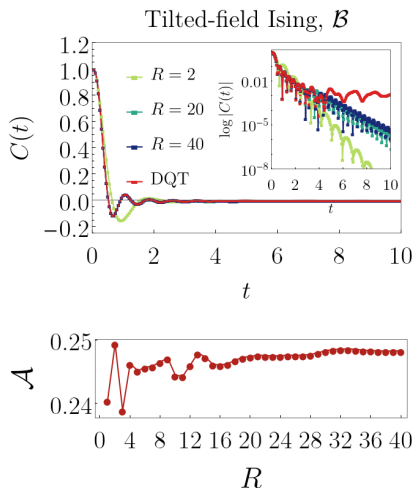


FIG. 5. **Top:** Comparison of the LP curves for the observable \mathcal{B} in the tilted-field Ising model against DQT data for the finite system with $L = 28$. **Bottom:** The areas under the curve of the LP approximation for different R . Here we find convergence at $R = 33$.

can be traced back to the observable at hand. The long-time behavior of \mathcal{J}_E follows a power law, see e.g. [16]. Therefore a description of the autocorrelation in terms of (few) damped oscillations is particularly unsuitable.

It is worth noticing that in each case, the minimal number of constituents is well below the technically feasible approximation by an approximation with $n_{\max}/2$ damped oscillations.

2D Ising model. Next, we examine a two-dimensional transverse field Ising model. Note that this precise set-

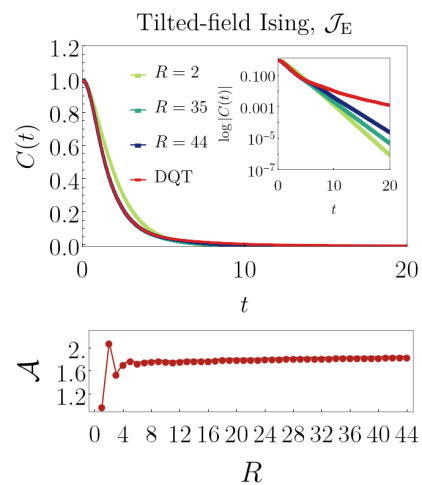


FIG. 6. **Top:** Comparison of the LP curves for the energy current \mathcal{J}_E in the tilted-field Ising model against DQT data for the finite system with $L = 28$. **Bottom:** The areas under the curve of the LP approximation for different R . Here we find convergence at $R = 35$.

up was previously studied in a related context [8]. The respective Hamiltonian is given by

$$\mathcal{H} = \sum_{\langle ij \rangle} \sigma_i^x \sigma_j^x + \sum_i \sigma_i^z. \quad (35)$$

Here, by the notation $\langle ij \rangle$ the sum is restricted to adjacent sites on the two-dimensional lattice. Again, the observable of interest is the respective energy current

$$\mathcal{J}_E^{2d} = \sum_{\langle ij \rangle | i < j} \sigma_i^x \sigma_j^y + \sigma_j^x \sigma_i^y, \quad (36)$$

where the sum extends over horizontal bonds, with site i always preceding site j . The first 21 Lanczos coefficients are taken from Ref. [8]. Here we do not compare with DQT results, because of the limits set by finite-size effects for two-dimensional systems, but with results obtained by solving the matrix equation (5). To this end, we considered the case where $\dim(\mathbf{L}) = 2^{18}$ by means of Chebyshev polynomials [17]. Note that this is the only instance in this paper where we need to perform a linear continuation of the Lanczos coefficients. Given 21 Lanczos coefficients, the LP approach constructs an approximation to $C(t)$ as a superposition of 10 damped oscillations and one exponential decay. The agreement to the autocorrelation function obtained from the 2^{18} -dimensional Liouvillian \mathbf{L} is remarkable, even on the log-scale.

V. HIGHER CORRELATORS

The LP scheme may be extended to not only apply to autocorrelation function $C(t) = \langle \mathcal{O} | e^{i\mathcal{L}t} | \mathcal{O} \rangle$, but also

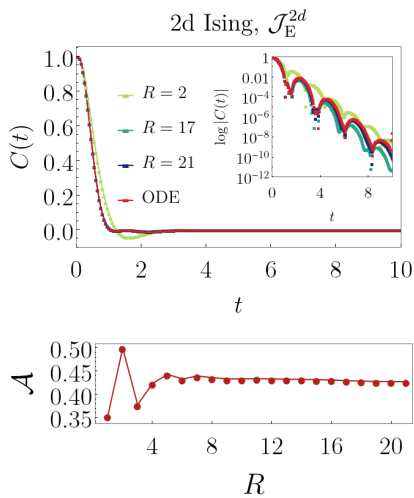


FIG. 7. **Top:** Comparison of the LP curves for the observable \mathcal{J}_E^{2d} in the 2d Ising model against the solution of the respective matrix equation (5) with $\dim(\mathbf{L}) = 2^{18}$. **Bottom:** The areas under the curve of the LP approximation for different R . Here we find convergence at $R = 17$.

to higher correlators. By considering the same differential equations (4), (5), altering the initial condition to $\varphi_n(0) = \delta_{n,j}$ to some $j \neq 0$ allows to study correlation functions of the initial operator with its derivatives. Concretely, $\varphi_n(0) = \delta_{n,1}$ amounts to

$$(\mathcal{O}_1(t)|\mathcal{O}_0) \sim \langle [\mathcal{H}, \mathcal{O}_0](t)|\mathcal{O}_0 \rangle. \quad (37)$$

Again, we compare the LP curves to DQT results. For reasons of conciseness, we restrict ourselves to the modes of the energy-density operators \mathcal{O} as well as to the two-local observable \mathcal{B} , see Fig. 8. Note that we stick to the nomenclature of Eqs. (37) and (2), to possibly avoid cluttering of notation. Again, the numerics show a high accuracy of our method. Concretely, we again find that the correlation functions given in Eq. (37) are remarkably well described by ~ 10 damped oscillations.

VI. CONCLUSION AND REMARKS

In this paper we investigated the apparent simple structure of correlation functions in complex quantum systems. To this end we expanded on a scheme in order to truncate the in principle infinite-dimensional Liouvillian to a small, finite matrix featuring a so-called truncation vector. This truncated Liouvillian gives rise to solutions for correlation functions in terms of a fixed number of exponentially damped oscillations. Moreover we argue that a good approximation of correlation functions in terms of few damped oscillations exists, given that the respective Lanczos coefficients attain a smooth growth after a number on the order of the number of the mentioned few damped oscillations. An explicit quantifier of this smoothness (that can be checked easily) is

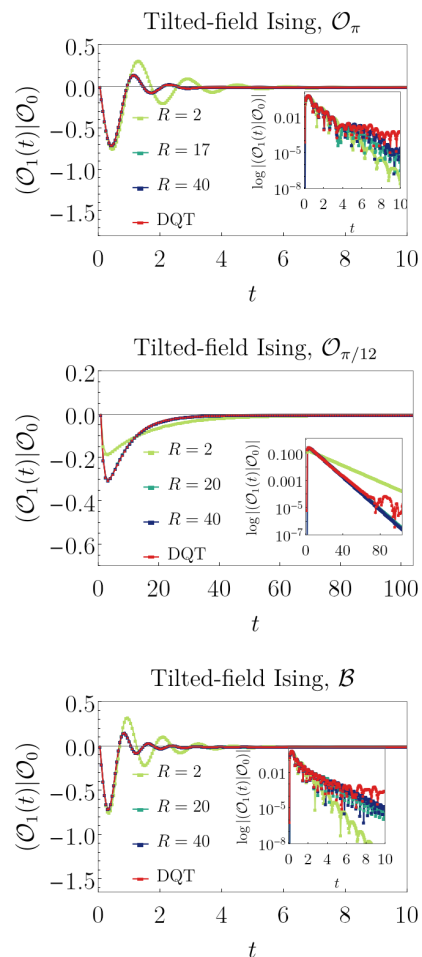


FIG. 8. **Top to bottom:** Correlation function of type $(\mathcal{O}_0|\mathcal{O}_1(t))$ for the fast and slow mode of the energy density-wave, \mathcal{O}_π and $\mathcal{O}_{\pi/12}$, as well as for the two-local observable \mathcal{B} .

given. While we only explicitly belabor the above existence argument for the Fourier transform of the correlation function at frequency $\omega = 0$, this argument can be extended in a somewhat more involved form to include finite frequencies. With the operator growth hypothesis that states that for infinite-dimensional chaotic quantum systems the Lanczos coefficients asymptotically attain linear growth, i.e., smooth growths, these arguments indicate that such an approximability is generic for chaotic quantum models. We investigated a frequently consulted toy model as well as two generic chaotic spin systems numerically. With the exception of observables that are known to feature power-law decay, we found remarkable accuracy of the LP scheme, hinting towards the genericness of simple dynamics in complex chaotic quantum systems.

ACKNOWLEDGMENTS

We thank Christian Bartsch, Robin Heveling and Mats Lamann for fruitful and valuable discussions. This work

has been funded by the Deutsche Forschungsgemeinschaft (DFG), under Grant No. 531128043, as well as under Grants No. 397107022, No. 397067869, and No. 397082825 within the DFG Research Unit FOR 2692, under Grant No. 355031190.

-
- [1] C. Gogolin and J. Eisert, Equilibration, thermalisation, and the emergence of statistical mechanics in closed quantum systems, *Rep. Prog. Phys.* **79**, 056001 (2016).
 - [2] L. D’Alessio, Y. Kafri, A. Polkovnikov, and M. R. and, From quantum chaos and eigenstate thermalization to statistical mechanics and thermodynamics, *Adv. Phys.* **65**, 239 (2016).
 - [3] J. M. Deutsch, Eigenstate thermalization hypothesis, *Rep. Prog. Phys.* **81**, 082001 (2018).
 - [4] R. Heveling, J. Wang, C. Bartsch, and J. Gemmer, Stability of exponentially damped oscillations under perturbations of the mori-chain, *J. Phys. Comm.* **6**, 085009 (2022).
 - [5] L. Dabelow and P. Reimann, Relaxation theory for perturbed many-body quantum systems versus numerics and experiment, *Phys. Rev. Lett.* **124**, 120602 (2020).
 - [6] T. Prosen and M. Žnidarič, Stability of quantum motion and correlation decay, *J. Phys. A: Math. Gen.* **35**, 1455 (2002).
 - [7] T. Mori, Liouvillian-gap analysis of open quantum many-body systems in the weak dissipation limit, *Phys. Rev. B* **109**, 064311 (2024).
 - [8] A. Teretenkov, F. Uskov, and O. Lychkovskiy, *Pseudomode expansion of many-body correlation functions* (2025), [arXiv:2407.12495 \[cond-mat.str-el\]](https://arxiv.org/abs/2407.12495).
 - [9] N. Loizeau, B. Buca, and D. Sels, *Opening krylov space to access all-time dynamics via dynamical symmetries* (2025), [arXiv:2503.07403 \[quant-ph\]](https://arxiv.org/abs/2503.07403).
 - [10] M. Lamann, *Influence of matrix structures in spin systems*, *Ph.D. thesis*, Universität Osnabrück (2024).
 - [11] D. E. Parker, X. Cao, A. Avdoshkin, T. Scaffidi, and E. Altman, A universal operator growth hypothesis, *Phys. Rev. X* **9**, 041017 (2019).
 - [12] C. Bartsch, A. Dymarsky, M. H. Lamann, J. Wang, R. Steinigeweg, and J. Gemmer, Estimation of equilibration time scales from nested fraction approximations, *Phys. Rev. E* **110**, 024126 (2024).
 - [13] J. Wang, M. H. Lamann, R. Steinigeweg, and J. Gemmer, Diffusion constants from the recursion method, *Phys. Rev. B* **110**, 104413 (2024).
 - [14] C. Joslin and C. Gray, Calculation of transport coefficients using a modified mori formalism, *Mol. Phys.* **58**, 789 (1986).
 - [15] C. Bartsch and J. Gemmer, Dynamical typicality of quantum expectation values, *Phys. Rev. Lett.* **102**, 110403 (2009).
 - [16] L. Capizzi, J. Wang, X. Xu, L. Mazza, and D. Poletti, Hydrodynamics and the eigenstate thermalization hypothesis, *Phys. Rev. X* **15**, 011059 (2025).
 - [17] Note that in Ref. [8] the comparison of the *pseudomode expansion* advocated there, was also performed against a solution of the respective matrix equation.